Superconducting qubit network with controllable nearest neighbor coupling

Superconducting qubit network with controllable nearest-neighbour coupling

New Journal of Physics
The open-access journal for physics

Superconducting qubit network with controllable nearest-neighbour coupling

M Wallquist, J Lantz, V S Shumeiko and G Wendin[1]
Department of Microtechnology and Nanoscience, Chalmers University of Technology, 41296 Gothenburg, Sweden
E-mail: wendin@mc2.chalmers.se

New Journal of Physics **7** (2005) 178
Received 15 March 2005
Published 26 August 2005
Online at http://www.njp.org/
doi:10.1088/1367-2630/7/1/178

Abstract. We investigate the design and functionality of a network of loop-shaped charge qubits with switchable nearest-neighbour coupling. The qubit coupling is achieved by placing large Josephson junctions (JJs) at the intersections of the qubit loops and selectively applying bias currents. The network is scalable and makes it possible to perform a universal set of quantum gates. The coupling scheme allows gate operation at the charge degeneracy point of each qubit, and also applies to charge-phase qubits. Additional JJs included in the qubit loops for qubit readout can also be employed for qubit coupling.

[1] Author to whom any correspondence should be addressed.

PII: S1367-2630(05)96417-3

Contents

1. Introduction

During the last six years it has been experimentally proven that superconducting circuits can serve as quantum mechanical two-level systems, qubits, to be used for quantum information processing [1]–[6]. Besides the experiments with individual qubits, several experiments have been performed so far on two permanently coupled qubits [7]–[11]. For instance, to observe the coupling of two charge qubits, the qubit islands have been permanently coupled via a capacitor, and the strength of the coupling has been varied by tuning the qubits in and out of resonance with each other (by varying the gate voltage) [7, 8].

In order to build a functional, scalable quantum computer, a network design is needed that allows coupling of an arbitrarily large number of qubits, with the possibility to switch on and off the coupling by means of external control knobs. In principle, coupling of only nearest-neighbour qubits is sufficient to perform a universal set of gates [12].

Theoretical schemes for variable coupling of charge qubits have been intensively discussed in literature. Couplings via inductive and capacitive elements have been examined as well as couplings via linear LC-oscillators and Josephson junctions (JJs) [13]–[17]. A standard approach to achieve a variable coupling is to employ a SQUID-type geometry either for the qubits [18] or for the coupling element [19], to be able to control the Josephson energy by an external magnetic flux. A somewhat different approach has been suggested in [20], where the qubits are coupled via another charge qubit thus creating a variable capacitive coupling.

Recently, a different way to achieve a variable inductive coupling has been suggested, namely to let the charge-qubit loops intersect and share a coupling JJ or SQUID. The interaction

is then controlled either by varying the magnetic flux in the qubit loops (or the coupling SQUID) [21], or by applying bias currents to the coupling JJ [22].

In this paper we give a detailed analysis of the qubit network based on the coupling method proposed in [22]. The idea of this method is to couple loop-shaped charge qubits by letting the circulating loop currents, which are sensitive to the charge state of the qubit island, interact. This is done by placing a nonlinear oscillator—a large JJ—at the intersection of the qubit loops. Such a coupling can be made variable by using the fact that in the absence of an external magnetic field, the persistent currents in the qubit loops are absent (for symmetric qubits with equal JJs). However, when a dc current bias is applied to a coupling JJ the symmetry is broken and currents start to circulate, the magnitude of the currents being dependent on the bias current. These currents interact with the oscillator, resulting in a variable effective qubit–qubit coupling. A similar coupling effect can be accomplished by inserting large readout JJs in the qubit loops [3]. As we show in this paper, applying current to one of the read-out junctions allows one to measure the state of the corresponding qubit without disturbing the other qubits (to first order); however, when two neighbouring read-out junctions are biased, the qubit–qubit coupling is switched on.

The advantage of the current-biased coupling scheme is that it does not need any local magnetic fields to control the coupling, fields which could create unwanted parasitic long-range interactions. An important feature is the possibility to operate at the qubit charge degeneracy point, where the decoherence effect is minimized [3, 23], and where the gate operations are very simple. This coupling scheme can also be extended to charge-phase qubits which are still less sensitive against decoherence due to flatter band structure [3]. With this coupling mechanism, neighbouring qubits in an arbitrarily long qubit chain can be coupled, and several independent two-qubit gates can be performed simultaneously. The fundamental entangling two-qubit gate is a control-phase (CPHASE) gate, which together with single-qubit gates constitute a universal set of operations.

The structure of the paper is as follows: in section 2 we explain the principles of the coupling by considering the simplest case of two coupled qubits. We estimate the maximum coupling strength, evaluate the residual parasitic couplings, and investigate the charge-phase regime for the qubits. In section 3 we add measurement junctions to the qubit circuits and investigate how to use these junctions as read-out devices and the means to create qubit coupling. In section 4 we generalize the derivation of section 3 to a multi-qubit network with an arbitrary number of coupled qubits. Finally, in section 5, we discuss how to use the network for quantum computing.

2. Controllable coupling of two qubits

To more clearly explain the principle of the qubit coupling, we first consider the case of two coupled qubits. The qubits consist of single Cooper pair boxes (SCB) with loop-shaped electrodes [3, 24]. To create coupling between the qubits, a large-capacitance JJ is placed at the intersection of the qubit loops, see figure 1. The physics of the coupling is as follows: as long as no magnetic flux is applied to the qubit loops, and no bias current is sent through the coupling junction, there are no circulating currents in the qubit loops. However, when the bias current is switched on, circulating currents start to flow in the clockwise or counter-clockwise direction depending on the charge state of the Cooper pair box. These currents displace the coupling junction oscillator and change its ground state energy, leading to an effective qubit–qubit interaction. The strength of the interaction is proportional to the bias current through the coupling junction. In the idle state,

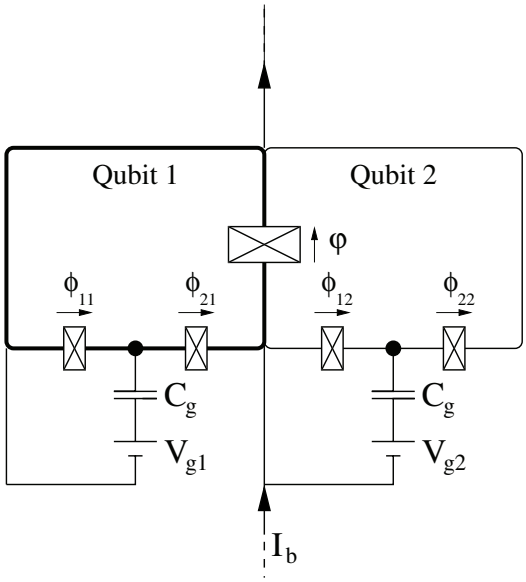

Figure 1. A system of two coupled charge qubits. V_{gi} control the individual qubits whereas I_b controls the coupling of the two qubits. Arrows indicate the direction of the Josephson current for positive phase difference (smaller than π).

when the bias current is switched off, small phase fluctuations at the coupling junction generate permanent parasitic qubit–qubit coupling. However, this parasitic coupling can be made small compared to the controllable coupling by choosing the plasma frequency of the coupling junction $\omega_b = (1/\hbar)\sqrt{2E_J^b E_C^b}$ to be small compared to the Josephson energy E_J^b. This requirement implies that the junction charging energy E_C^b must be small,

$$E_C^b \ll \hbar\omega_b \ll E_J^b, \tag{1}$$

i.e. the coupling junction must be in the phase regime. This is the most essential requirement for the qubit coupling under consideration.

2.1. Circuit Hamiltonian

We begin the evaluation of qubit coupling with the derivation of a circuit Hamiltonian. To this end, we first write down the Lagrangian L of the circuit in figure 1. The Lagrangian consists of the respective Lagrangians of the SCBs and the coupling JJ,

$$L = \sum_{i=1}^{2} L_{\mathrm{SCB},i} + L_{\mathrm{JJ}}. \tag{2}$$

Assuming the SCB to consist of identical junctions with capacitance C and Josephson energy E_J, and following the rules described in e.g. [25, 26], we write the corresponding Lagrangian in the form,

$$L_{\mathrm{SCB},i} = \frac{\hbar^2 C}{2(2e)^2}(\dot{\phi}_{1i}^2 + \dot{\phi}_{2i}^2) + \frac{\hbar^2 C_g}{2(2e)^2}\left(\frac{2e}{\hbar}V_{gi} - \dot{\phi}_{1i}\right)^2 + E_J(\cos\,\phi_{1i} + \cos\,\phi_{2i}), \tag{3}$$

where ϕ_{1i} (ϕ_{2i}) is the phase difference across the left (right) JJ of the ith SCB, and C_g is the gate capacitance. The Lagrangian of the coupling JJ includes the electrostatic energy and the Josephson energy of the junction, and also the interaction energy of the junction with applied bias current I_b,

$$L_{\mathrm{JJ}} = \frac{\hbar^2 C_b}{2(2e)^2}\dot{\varphi}^2 + E_J^b \cos\,\varphi + \frac{\hbar}{2e} I_b \varphi, \tag{4}$$

where φ is the phase difference across the coupling junction.

The flux quantization condition in each of the qubit loops allows the elimination of one of the qubit variables from the Lagrangian. We assume that there is no external magnetic flux in the loops since magnetic flux will not be used to control either the qubits or the qubit interaction, and we also assume that the loop self-inductances are negligible. Then the flux quantization equation takes the form,

$$\phi_{+,1} + \varphi = 0, \qquad \phi_{+,2} - \varphi = 0. \tag{5}$$

where we introduced new qubit variables,

$$\phi_{-,i} = \tfrac{1}{2}(\phi_{2i} - \phi_{1i}), \qquad \phi_{+,i} = \phi_{1i} + \phi_{2i}. \tag{6}$$

By virtue of relations (5), the gate capacitance terms will take the form $(\hbar^2 C_g/2(2e)^2)(2eV_{gi}/\hbar + \dot{\phi}_{-,i} \pm \dot{\varphi}/2)^2$ introducing a capacitive interaction of the SCB with the coupling junction. From here on, the upper (lower) sign corresponds to the first (second) qubit. Similarly, the appearance of the variable φ in the SCB Josephson terms introduces an inductive interaction between the SCB and the coupling junction.

At this point, we are ready to proceed to the circuit Hamiltonian. By introducing the conjugated variables, $n_i = (1/\hbar)(\partial L/\partial\dot{\phi}_{-,i})$, and $n = (1/\hbar)(\partial L/\partial\dot{\varphi})$, which have the meaning of dimensionless charges (in the units of Cooper pairs) on the SCB and on the island confined between the coupling JJ and the SCBs, respectively, and then applying the Legendre transformation, $H = \sum_i \hbar\, n_i\dot{\phi}_{-,i} + \hbar\, n\dot{\varphi} - L$, we get,

$$H = \sum_{i=1}^{2} H_{\mathrm{SCB},i} + H_{\mathrm{JJ}} + H_C. \tag{7}$$

Here

$$H_{\mathrm{SCB},i} = E_C(n_i - n_{gi})^2 - 2E_J \cos\frac{\varphi}{2}\cos\,\phi_{-,i}, \tag{8}$$

is the SCB Hamiltonian, where $E_C = (2e)^2/2C_\Sigma$, $C_\Sigma = 2C + C_g$ is the total capacitance of the qubit island and $n_{gi} = C_g V_{gi}/2e$ is the (dimensionless) charge induced on the qubit island by the gate voltage. The JJ Hamiltonian is

$$H_{\mathrm{JJ}} = E_C^b\left(n - \frac{n_{g1} - n_{g2}}{2}\right)^2 - E_J^b \cos\,\varphi - \frac{\hbar}{2e} I_b \varphi, \tag{9}$$

where $E_C^b = (2e)^2/(2C_b + C_\Sigma)$. The last term in equation (7),

$$H_C = \frac{C_g}{C_\Sigma} E_C^b \left(n - \frac{n_{g1} - n_{g2}}{2} \right) ((n_2 - n_{g2}) - (n_1 - n_{g1})) - \frac{C_g^2}{2C_\Sigma^2} E_C^b (n_1 - n_{g1})(n_2 - n_{g2}), \tag{10}$$

describes capacitive interaction of the qubits and the JJ, and also direct qubit–qubit coupling, induced by the gate capacitance.

The Hamiltonian (7) is quantized by imposing the canonical commutation relations, $[\phi_{-,j}, n_k] = \mathrm{i}\delta_{jk}$, $[\varphi, n] = \mathrm{i}$. To incorporate the Coulomb blockade effect, we take advantage of the periodic SCB potential and impose periodic boundary conditions on the wave function with respect to the phase $\phi_{-,i}$. This results in charge quantization on the island. Keeping the system at low temperature ($k_B T < E_C$) and close to the charge degeneracy point $n_g = 1/2$, restricts the number of excess charges on the island to zero or one Cooper pair. Assuming the charge regime, $E_C \gg E_J$ for the SCB, and no transitions to the higher charge states to occur during qubit operation, we truncate the SCB Hilbert space to these two lowest charge states. Then the single-qubit Hamiltonian reads

$$H_i = \frac{E_C}{2}(1 - 2n_{gi})\sigma_{zi} - E_J \cos\frac{\varphi}{2}\sigma_{xi}, \tag{11}$$

while the capacitive interaction (10) takes the form,

$$H_C = \frac{C_g}{2C_\Sigma} E_C^b \left(n - \frac{n_{g1} - n_{g2}}{2} \right) (\sigma_{z2} - \sigma_{z1}) - \frac{C_g^2}{8C_\Sigma^2} E_C^b \sigma_{z1}\sigma_{z2}. \tag{12}$$

The qubits and JJ both interact capacitively, equation (12), and inductively (the last term in equation (11)). It has been noticed by Shnirman *et al* [13], that the capacitive interaction can be fully transformed into an inductive one. This can be done by using a unitary rotation conveniently combined with a gauge transformation eliminating the gate-charge-dependent terms in equations (12) and (9) (this is possible since the charge on the coupling JJ is not quantized). The corresponding unitary operator is

$$U = \exp\left[-\mathrm{i}\alpha(\sigma_{z2} - \sigma_{z1})\varphi\right] \exp\left(\mathrm{i}\frac{n_{g1} - n_{g2}}{2}\varphi\right), \qquad \alpha = \frac{C_g}{4C_\Sigma}. \tag{13}$$

It is straightforward to check that the transformed part of the Hamiltonian, $U^\dagger(H_{\mathrm{JJ}} + H_C)U$, does not contain any interaction, while the whole interaction is concentrated in the Josephson term of the qubit Hamiltonian,

$$U^\dagger H_i U = \frac{E_C}{2}(1 - 2n_{gi})\sigma_{zi} - E_J \cos\frac{\varphi}{2}[\cos(2\alpha\varphi)\sigma_{xi} \pm \sin(2\alpha\varphi)\sigma_{yi}]. \tag{14}$$

The α-dependent correction is small when the gate capacitance is small, $C_g \ll C_\Sigma$.

2.2. *Controllable qubit coupling*

Let us consider the main part of the inductive interaction. Making use of assumption, equation (1), we consider small phase fluctuations across the JJ, $\gamma = \varphi - \varphi_0$, around the minimum point φ_0,

and expand the φ-dependent terms in equation (14) in powers of $\gamma \ll 1$. The quantity φ_0 is determined by the applied bias current I_b,

$$\sin\varphi_0 = \frac{\hbar I_b}{2eE_J^b}. \tag{15}$$

To zeroth order with respect to γ we get a free qubit Hamiltonian which, after additional rotation $U' = \exp[i\alpha(\sigma_{z2} - \sigma_{z1})\varphi_0]$, takes the form,

$$H_i = \frac{E_C}{2}(1 - 2n_{gi})\sigma_{zi} - E_J \cos\frac{\varphi_0}{2}\sigma_{xi}. \tag{16}$$

Controllable qubit–qubit coupling results from the terms which are linear in γ in the expansion of equation (14). Neglecting the effect of the small α in these terms (which will be considered in the next section), we obtain,

$$H_{\text{int}} = \frac{1}{2}E_J \sin\frac{\varphi_0}{2}\gamma(\sigma_{x1} + \sigma_{x2}). \tag{17}$$

It is convenient to combine these terms with the quadratic potential of the JJ that approximates the tilted Josephson potential near its minimum. We then get the total Hamiltonian in the form,

$$H = \sum_i H_i - \lambda E_J \frac{\sin^2(\varphi_0/2)}{4\cos\varphi_0}\sigma_{x1}\sigma_{x2} + H_{\text{osc}}, \tag{18}$$

where $\lambda = E_J/E_J^b$, and

$$H_{\text{osc}} = E_C^b n^2 + \frac{1}{2}E_J^b \cos\varphi_0 \left[\gamma + \lambda\frac{\sin(\varphi_0/2)}{2\cos\varphi_0}(\sigma_{x1} + \sigma_{x2})\right]^2 \tag{19}$$

is the Hamiltonian of a displaced linear oscillator associated with the coupling JJ.

The further analysis is significantly simplified if one assumes the qubit–oscillator interaction to be small, $\lambda \ll 1$, and the oscillator to be fast on a time scale of qubit evolution, $\hbar\omega_b \gg E_J$. In fact, these assumptions are not needed when the qubits are parked at the charge degeneracy point, $n_{gi} = 1/2$, because in this case the interaction term commutes with the qubit Hamiltonians, and the problem is exactly solvable [27]. The assumption on λ can be relaxed for the two-qubit circuit; however for a multi-qubit network it becomes essential, as discussed later.

The imposed constraints together with equation (1) lead to the following chain of inequalities:

$$E_J \ll \hbar\omega_b \ll E_J^b. \tag{20}$$

Under these constraints, one can neglect the excitation of the oscillator, which at low temperature will remain in the ground state. This does not significantly differ from the ground state of the Hamiltonian in equation (19). For instance, the estimate for the amplitude of the first order correction reads,

$$c_{0\to1} \sim \frac{E_C(1 - 2n_g)}{(\hbar\omega_b E_J^b)^{1/2}(\cos\varphi_0)^{3/4}} \sim \frac{E_J}{(\hbar\omega_b E_J^b)^{1/2}} \ll 1. \tag{21}$$

Therefore one can average over the oscillator ground state and drop the oscillator energy term, because it does not depend on the qubit-state configurations.

Summarizing our derivation, after integrating out the oscillator, we arrive at the effective two-qubit Hamiltonian,

$$H_{\rm eff} = \sum_i H_i - \lambda E_J \frac{\sin^2(\varphi_0/2)}{4\cos\varphi_0}\sigma_{x1}\sigma_{x2}. \tag{22}$$

The qubit–qubit coupling term in equation (22) has a clear physical meaning: it results from interacting persistent currents in the qubit loops. Indeed, the persistent currents are given in terms of equations (3)–(8) by the relation $I_i = (2e/\hbar)E_J \sin(\phi_{1i})$, or identically,

$$I_i = \frac{2e}{\hbar}E_J \sin\frac{\phi_{+,i}}{2}\cos\phi_{-,i} = \frac{2e}{\hbar}\frac{\partial H}{\partial\phi_{+,i}}. \tag{23}$$

In the truncated form, this relation reduces to

$$I_i = \frac{e}{\hbar}E_J \sin\frac{\varphi_0}{2}\sigma_{xi} \tag{24}$$

(neglecting phase fluctuations over the coupling JJ), and the coupling term in equation (22) can be expressed as an inductive coupling energy of the two persistent currents, $L_b I_1 I_2$, with the Josephson inductance of the tilted coupling junction,

$$L_b = \frac{\hbar^2}{4e^2 E_J^b \cos\varphi_0}, \tag{25}$$

playing the role of mutual inductance. In the absence of the bias current when the JJ potential is not tilted, $\sin\varphi_0 = 0$, the persistent currents are not excited and the coupling is switched off. When the bias current is applied, the coupling is switched on, and its strength increases with the bias current because of increasing persistent currents, and also because of decreasing JJ inductance.

2.3. Effect of qubit asymmetry

Let us consider the effect of small α-terms in equation (14). Although small, the last term in this equation proportional to σ_y leads to an interesting qualitative effect in the qubit coupling, changing its symmetry. A similar effect is produced by asymmetry of the qubit junctions. Although an ideal qubit should consist of identical JJs, in practice the junction parameters may vary at least within the range of a few per cent. In the asymmetric case, the property of the symmetric qubit to have zero persistent current when the bias is turned off is lost. Now a persistent current is spontaneously generated, the direction of which depends on the charge state of the SCB. This affects the symmetry of the controllable qubit coupling.

The most important is the variation of the Josephson energy. For an asymmetric qubit, the Josephson term in Lagrangian, equation (3), has the form, $E_{J1}\cos\phi_{1i} + E_{J2}\cos\phi_{2i}$. For small junction asymmetry, $\delta E_J = E_{J1} - E_{J2} \ll E_J$, the Josephson term in the qubit Hamiltonian, equation (11), acquires the form

$$-E_J \cos\frac{\varphi}{2}\sigma_{xi} \pm \frac{\delta E_J}{2}\sin\frac{\varphi}{2}\sigma_{yi}. \tag{26}$$

The second term in this equation, resulting from the junction asymmetry, has the same y-symmetry as the last term in equation (14). They can therefore be considered on the same footing and added to the interaction Hamiltonian (17), which now takes the form,

$$H_{\rm int} = E_J\gamma\left[\frac{1}{2}\sin\frac{\varphi_0}{2}(\sigma_{x1}+\sigma_{x2}) + \cos\frac{\varphi_0}{2}\left(2\alpha - \alpha\varphi_0\tan\frac{\varphi_0}{2} - \frac{\delta E_J}{4E_J}\right)(\sigma_{y2}-\sigma_{y1})\right]. \tag{27}$$

The additional terms give rise to a small direct qubit coupling of the xy-type, in addition to the controllable xx-coupling in equation (22),

$$\frac{1}{4}\lambda E_J\tan\varphi_0\left(2\alpha - \alpha\varphi_0\tan\frac{\varphi_0}{2} - \frac{\delta E_J}{4E_J}\right)(\sigma_{y1}\sigma_{x2} - \sigma_{x1}\sigma_{y2}). \tag{28}$$

Although small, this additional coupling term does not commute with the qubit Hamiltonian even at the degeneracy point, which may complicate the gate operation discussed towards the end of this paper.

2.4. Residual qubit coupling

Even in the absence of bias current, and in the symmetric qubits, there exist small circulating currents in the qubit loops because of ground state phase fluctuation in the coupling junction. These currents interact via the coupling junction, creating a small parasitic coupling of the qubits. The effect is described by the higher order terms neglected in the previous discussion. One term, which does not vanish at $\varphi_0 = 0$ is due to the interaction via the gate capacitance (cf equation (27)),

$$H^{(1)}_{\rm int} = 2\alpha E_J\cos\frac{\varphi_0}{2}\gamma\,(\sigma_{y2}-\sigma_{y1}). \tag{29}$$

This term is linear in γ, and it creates a direct parasitic qubit–qubit coupling via the mechanism discussed in the previous sections,

$$H^{(1)}_{\rm res} = 4\alpha^2\lambda E_J\frac{\cos^2(\varphi_0/2)}{\cos\varphi_0}\sigma_{y1}\sigma_{y2}. \tag{30}$$

This coupling is smaller than the controllable coupling by a factor $\alpha^2 = (C_g/4C_\Sigma)^2 \ll 1$.

Obviously, the effect of the junction asymmetry also contributes to this kind of residual coupling, and can be included in equation (30), by making a change, $\alpha \to \alpha - \delta E_J/2E_J$.

Another parasitic term is quadratic in γ,

$$H^{(2)}_{\rm int} = \frac{1}{8}\lambda E^b_J\cos\frac{\varphi_0}{2}\gamma^2(\sigma_{x1}+\sigma_{x2}). \tag{31}$$

The effect of this interaction is to change the frequency, and hence the ground state energy of oscillator (19), depending on the qubit-state configuration. This squeezing effect creates a direct residual qubit coupling in the lowest-order approximation,

$$H^{(2)}_{\rm res} = -\frac{1}{128}\lambda E_J\frac{\hbar\omega_b}{E^b_J}\frac{\cos^2(\varphi_0/2)}{(\cos\varphi_0)^{3/2}}\sigma_{x1}\sigma_{x2}. \tag{32}$$

This coupling is smaller than the controllable interaction in equation (22) by a factor, $\hbar\omega_b/E^b_J \ll 1$.

2.5. Maximum coupling strength

Because of the limitation on the gate operation time imposed by decoherence, it is desirable that the qubit coupling is as strong as possible. In our case, the coupling strength is generally determined by the parameter λ; the strength however increases with the applied current bias. This is reflected by a cosine-factor in the denominator in equation (22), which formally turns to zero at $\varphi_0 = \pi/2$. This corresponds to the point when the bias current approaches the critical current value for the coupling JJ. At this point the minimum in the tilted Josephson potential disappears, and the junction switches to the resistive state, sweeping the qubit phase and thus destroying the qubit. Therefore the ultimate limitation on the coupling strength is imposed by the switching of the coupling JJ. The latter may even occur at smaller applied current because of tunnelling through the Josephson potential barrier (macroscopic quantum tunnelling, MQT). The assumption of a small MQT rate imposes an additional limitation on the coupling strength to the one imposed by the constraints (20). Indeed, because the potential wells of the tilted Josephson potential become shallow with decreasing Josephson energy, $E_J^b \cos\varphi_0$, the constraints must be reconsidered,

$$E_J \ll \hbar\omega_b\sqrt{\cos\varphi_0} \ll E_J^b \cos\varphi_0, \tag{33}$$

clearly putting limitations on the maximum allowed tilt.

In order to roughly estimate an upper bound for the maximum coupling strength, let us soften requirements (33), and consider the relations

$$E_J \sim \hbar\omega_b\sqrt{\cos\varphi_0} \sim E_J^b \cos\varphi_0. \tag{34}$$

Both the relations can be fulfilled by applying a sufficiently large bias current, and by choosing appropriate plasma frequency. The latter can be adjusted by shunting the coupling JJ with a large capacitance. The corresponding relations read,

$$\cos\varphi_0 \sim \frac{E_J}{E_J^b}, \qquad \hbar\omega_b \sim \sqrt{E_J E_J^b}. \tag{35}$$

The coupling strength for a tilted JJ is given by the phase-dependent coupling parameter in equation (22),

$$\lambda(\varphi_0) = \lambda\,\frac{\sin^2(\varphi_0/2)}{4\cos\varphi_0}. \tag{36}$$

The maximum value of this parameter is estimated by using equation (35),

$$\max\lambda(\varphi_0) \sim 1. \tag{37}$$

Let us compare this result with the limitation imposed by MQT. For a large applied bias current, the potential well can be approximated with a cubic curve, and the MQT rate is estimated by [30]

$$\Gamma_{\mathrm{MQT}} = \omega_b\sqrt{\frac{30s}{\pi}\cos\varphi_0}\,\mathrm{e}^{-s}, \qquad s = \frac{24E_J^b}{5\hbar\omega_b}\frac{(\cos\varphi_0)^{5/2}}{\sin^2\varphi_0}. \tag{38}$$

Suppose that the value $\hbar\omega_b \sim (1/2)E_J^b(\cos\varphi_0)^{5/2}$ gives a satisfactory small MQT rate ($\sim 10^{-4}E_J$ according to the following estimates). Under this condition, which is more restrictive than the right one in equation (34), the relations in equation (35) become modified,

$$\cos\varphi_0 \sim \left(\frac{E_J}{E_J^b}\right)^{1/3}, \qquad \hbar\omega_b \sim E_J^{5/6}(E_J^b)^{1/6}, \tag{39}$$

leading to a somewhat smaller maximum coupling parameter,

$$\max\lambda(\varphi_0) \sim \left(\frac{E_J}{E_J^b}\right)^{2/3} < 1. \tag{40}$$

2.6. Charge-phase regime

So far, we have assumed the qubit island to be in the charge regime $E_C \gg E_J$, where the two lowest charge eigenstates, $|n=0\rangle$ and $|n=1\rangle$, serve as the qubit basis. However, from an experimental point of view, it may be more appealing to work in the charge-phase regime $E_C \sim E_J$ because the qubit becomes more stable against charge noise when the energy bands flatten [3]. In this regime, the qubit states are given by Bloch wavefunctions, consisting of superpositions of many charge states. Nevertheless, as easily seen, the controllable qubit coupling via a current-biased large JJ will persist also in the charge-phase regime. Indeed, an essential physical characteristic of the qubit–JJ interaction is the persistent current in the qubit loop, equation (23), $I = (2e/\hbar)\sin(\phi_+/2)\cos\phi_-$. The magnitude of this current is controlled by the tilt of the JJ ($\sin(\phi_+/2) = \sin(\varphi_0/2)$), and it is zero when the JJ is idle, regardless of whether the qubit is in the charge or charge-phase regime.

Furthermore, an important property of the charge regime is that the qubit–JJ interaction is diagonal in the qubit eigenbasis when the qubit is parked at the charge degeneracy point, $n_g = 1/2$, i.e. it has zz-symmetry in this eigenbasis. This property simplifies the 2-qubit gate operations discussed later, and it also allows a quantum non-demolishing measurement of the qubit by means of current detection using the large JJ, as discussed in the next section. We show in this section that this property persists in the charge-phase regime. Namely, we show that the SCB Hamiltonian truncated to a pair of lowest Bloch states commutes with the truncated current operator at $n_g = 1/2$. This leads to direct qubit–qubit coupling of zz-type in the qubit eigenbasis.

Let us consider the SCB Hamiltonian $H_{\rm SCB}$, equation (8), in the charge basis, $|n\rangle$, and separate the part which does not depend on the gate charge,

$$H_1 = \sum_{n=-\infty}^{\infty} [E_C n(n-1)|n\rangle\langle n| - \tilde{E}_J(|n+1\rangle\langle n| + |n-1\rangle\langle n|)], \tag{41}$$

from a small part proportional to the departure from the charge degeneracy point (e.g. during single-qubit manipulation) $\delta n_g(t) = 1/2 - n_g(t)$,

$$H_2 = \sum_{n=-\infty}^{\infty} 2E_C\delta n_g(t) n|n\rangle\langle n|, \qquad H_{\rm SCB} = H_1 + H_2. \tag{42}$$

The notation $\tilde{E}_J = 2E_J \cos(\varphi/2)$ is introduced here for brevity. We split the complete set of the charge eigenstates, $-\infty < n < \infty$, in the positive and negative charge subsets labelled with $\sigma = \uparrow, \downarrow$, and m, $1 < m < \infty$, such that

$$\begin{array}{ll} m = n, & n > 0, \\ m = 1 - n, & n \leqslant 0. \end{array} \tag{43}$$

In the basis $|m, \sigma\rangle$, $m = \ldots, 2, 1$, the Hamiltonian H_1 acquires the form,

$$H_1 = \left[\begin{array}{c|c} H_0 & -\tilde{E}_J U \\ \hline -\tilde{E}_J U & H_0 \end{array}\right], \tag{44}$$

where H_0 is tridiagonal, and U contains only a single element,

$$H_0 = \begin{bmatrix} \ddots & \ddots & & \\ \ddots & 6E_C & -\tilde{E}_J & \\ & -\tilde{E}_J & 2E_C & -\tilde{E}_J \\ & & -\tilde{E}_J & 0 \end{bmatrix}, \qquad U = \begin{bmatrix} \ddots & & \vdots \\ & 0 & 0 \\ \ldots & 0 & 1 \end{bmatrix}. \tag{45}$$

A Hadamard rotation, H, in σ-space,

$$\mathrm{H} = \frac{1}{\sqrt{2}}(\sigma_z + \sigma_x), \tag{46}$$

takes the basis $|m\uparrow\rangle$, $|m\downarrow\rangle$ to $|m\pm\rangle = (1/\sqrt{2})(|m\uparrow\rangle \pm |m\downarrow\rangle)$, and transforms the matrix in equation (44),

$$H_1 = H_0\mathbf{1} - \tilde{E}_J U\sigma_x \to H_0\mathbf{1} - \tilde{E}_J U\sigma_z. \tag{47}$$

Then this matrix acquires a block-diagonal form,

$$H_1 = \left[\begin{array}{cc|cc} & & & \\ & H_0 - \tilde{E}_J U & & 0 \\ & & & \\ & \times & & \\ \hline & & & \\ & 0 & & H_0 + \tilde{E}_J U \\ & & & \\ & & & \times \end{array}\right]. \tag{48}$$

The above block-diagonal form is suitable for identifying the qubit states in the charge-phase regime. Indeed, when the Josephson energy is tuned to zero, the lower-corner elements of the blocks, marked with $\times$, correspond to the lowest energy states of the SCB. In fact, the Hadamard transformation (46) corresponds to the rotation to the eigenbasis of a charge qubit at the charge degeneracy point, which coincides with the current eigenbasis. When the Josephson energy increases, the eigenstates of the matrix (48) become superpositions of many charge states, which however does not mix the charge superpositions denoted with indices + and −, and can be obtained by independent rotations of the matrix blocks. During these rotations, although the two lower-corner eigenvalues marked with $\times$ do change, they however remain the lowest energy levels. This follows from the fact that the eigenvalues of the Mathieu equation do not cross when

the amplitude of the potential increases [28]. Therefore the charge qubit eigenstates develop to the lowest energy Bloch states, which are identified as the charge-phase qubit eigenbasis $|E_+\rangle$ and $|E_-\rangle$.

Let us evaluate the form of the current operator, equation (23), in the charge-phase qubit eigenbasis. The current operator in the charge representation is proportional to the operator $X = |n+1\rangle\langle n| + |n-1\rangle\langle n|$. In the $|m\sigma\rangle$-basis, this operator is written as

$$X = X_0\mathbf{1} + U\sigma_x, \tag{49}$$

where

$$X_0 = \begin{bmatrix} & \ddots & & & \\ \ddots & & 1 & & \\ & 1 & 0 & 1 & \\ & & 1 & 0 & \end{bmatrix}. \tag{50}$$

In the eigenbasis of H_1, i.e. after the Hadamard transformation, this operator acquires a block-diagonal form,

$$X \to \left[\begin{array}{c|c} X_0 + U & 0 \\ \hline 0 & X_0 - U \end{array}\right], \tag{51}$$

which means that X does not couple the states $|E_+\rangle$ and $|E_-\rangle$.

One implication of this result is that the qubit–qubit coupling in the charge-phase regime will still be of zz-type in the truncated Hilbert space, i.e. diagonal in the qubit eigenbasis. It also means that current measurement will not mix the qubit states, i.e., current detection provides a means for quantum non-demolition measurements.

Finally, we analyse the term H_2 in equation (42), which is non-zero only when the gate charge deviates from the degeneracy point. In the $|m\sigma\rangle$ representation, this term has the form,

$$H_2 = 2E_C\delta n_g(t)\left[\begin{array}{c|c} D_\uparrow & 0 \\ \hline 0 & D_\downarrow \end{array}\right], \tag{52}$$

where $D_\uparrow$ and $D_\downarrow$ are diagonal matrices,

$$D_\uparrow = \mathrm{diag}(\ldots, 3, 2, 1), \qquad D_\downarrow = \mathrm{diag}(\ldots, -2, -1, 0). \tag{53}$$

After the Hadamard rotation, it acquires the form,

$$H_2 \to E_C\delta n_g(t)\left[\begin{array}{c|c} \mathbf{1} & D_\uparrow - D_\downarrow \\ \hline D_\uparrow - D_\downarrow & \mathbf{1} \end{array}\right]. \tag{54}$$

Thus after truncation to the qubit basis, $D_\uparrow - D_\downarrow$ provide off-diagonal elements, which couple the qubit states and can be employed for qubit manipulation.

3. Coupling via read-out junctions

The read-out circuit is an important ingredient of the qubit network, which must be explicitly included in the consideration. We discuss here the read-out method successfully tested on a

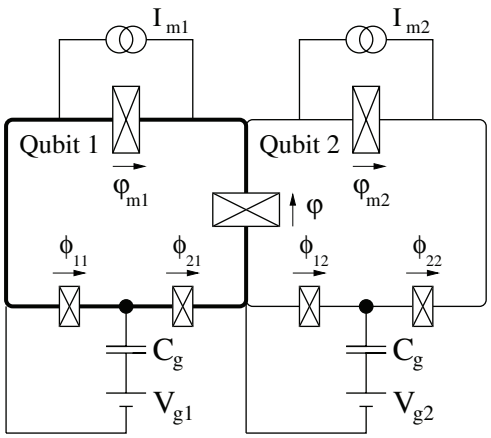

Figure 2. Applied currents I_{mi} across large measurement JJs can be used for reading out the current state of qubit i and for qubit coupling. Arrows indicate the direction of the Josephson current for positive phase difference (smaller than π).

single qubit by the Saclay group [3]. With this method, the persistent current flowing in the qubit loop is excited and measured by using a large JJ in the qubit loop, as shown in figure 2. To do the measurement, a large dc current is applied to the junction so that the net current through the junction either exceeds the critical value or not, depending on the direction of the persistent current in the loop. In the former case, the measurement JJ switches to a resistive state, which is detected by measuring a dc voltage across the JJ; in the latter case, no voltage is detected. This method of threshold detection is quite invasive, sweeping the phase across the qubit and creating a large number of quasi-particles. A recently tested more gentle method [29] utilizes an ac driving current with comparatively small amplitude applied to the JJ, and measures the qubit-state-dependent ac response.

We now analyse the compatibility of such measurement methods, via a large JJ, with our coupling scheme. Before proceeding with the calculations we note that one may distinguish two cases: measurement and coupling. In the measurement case, the bias current is applied only to a single measurement junction. This will excite the persistent current in the corresponding qubit loop, allowing qubit readout, while the neighbouring qubit loop will remain, as we will see, in the idle state, neglecting the effect of a small parasitic coupling, and this qubit will not be destroyed. In the coupling case, bias current sent through both measurement junctions in figure 2 will create persistent currents in both qubit loops, resulting in the qubit coupling discussed above. This physical picture implies that qubit–qubit coupling can be achieved even without sending current through the coupling junction [22].

3.1. Measurement of individual qubits

When a measurement JJ is included in each qubit loop (figure 2), the corresponding terms must be added to the circuit Lagrangian equation (2):

$$L_{mi} = \frac{\hbar^2 C_{mi}}{2(2e)^2}\dot{\varphi}_{mi}^2 + E_{Ji}^m \cos\varphi_{mi} + \frac{\hbar}{2e} I_{mi}\varphi_{mi}. \tag{55}$$

Here φ_{mi} denotes the phase across the measurement junction of the ith qubit, and I_{mi} is the applied current. The phase quantization relations (5) will now change,

$$\phi_{+,1} + \varphi - \varphi_{m1} = 0, \qquad \phi_{+,2} - \varphi - \varphi_{m2} = 0, \tag{56}$$

giving rise to interaction of the qubits with the measurement JJ, in addition to the coupling JJ, in the charge sector as well as in the current sector. As before, it is possible to eliminate the capacitive interaction, but now it is more convenient to do it on the Lagrangian level. The interaction via the gate capacitance is eliminated via transformation of the qubit variable,

$$\phi_{-,i} \to \phi_{-,i} + 2\alpha(\varphi_{mi} \mp \varphi), \tag{57}$$

which is equivalent to the transformation in equation (13) (the upper (lower) sign corresponds to the first (second) qubit). As already described, this interaction leads to a small residual direct yy-qubit coupling, which we will omit from the further discussion. Similarly, the capacitive interaction via the qubit capacitance C can be eliminated by transformation of the measurement JJ variable,

$$\varphi_{mi} \to \varphi_{mi} \pm \beta\varphi, \qquad \beta = \frac{C}{2C_{mi} + C}. \tag{58}$$

This transformation will only slightly affect the inductive interaction since β is small.

At this point, we proceed to the quantum description of the circuit and truncate the qubit Hamiltonian, assuming the charge regime, $E_C \gg E_J$. The circuit Hamiltonian will take the form,

$$H = \sum_{i=1}^{2}(H_i + H_{mi}) + H_{\mathrm{JJ}}, \tag{59}$$

where

$$H_i = \frac{E_C}{2}(1 - 2n_{gi})\sigma_{zi} - E_J \cos\frac{(1-\beta)\varphi \mp \varphi_{mi}}{2}\,\sigma_{xi}, \tag{60}$$

refers to the qubits, while

$$H_{mi} = E^m_{Ci} n^2_{mi} - E^m_{Ji}\cos(\varphi_{mi} \pm \beta\varphi) - \frac{\hbar}{2e} I_{mi}(\varphi_{mi} \pm \beta\varphi), \tag{61}$$

and

$$H_{\mathrm{JJ}} = E^b_C n^2 - E^b_J \cos\varphi, \tag{62}$$

are the Hamiltonians of the measurement JJ and the coupling JJ, respectively. In these equations, $E^m_{Ci} = (2e)^2/(2C_{mi} + C)$, and $E^b_C = (2e)^2/2C_{b\Sigma}$, $C_{b\Sigma} = C_b + \sum_i [C(C_{mi} + C)/(2C_{mi} + C)]$; the current applied to the coupling junction is absent because we will focus on the effect of the measurement junctions.

In the measurement regime, only a single external current, say I_{m1}, is applied. The steady-state point for the 3-JJ network, $(\varphi_0, \varphi_{mi,0})$, is found from equations (60)–(62) in the main

approximation with respect to the small parameters $\beta \approx C/C_b$ and $\lambda = E_J/E_J^b$,

$$\sin\varphi_{m1,0} = \frac{\hbar}{2e}\frac{I_{m1}}{E_{J1}^m}, \qquad \varphi_0 = \frac{\lambda}{2}\sin\frac{\varphi_{m1,0}}{2}\sigma_{x1}, \qquad \varphi_{m2,0} = \beta\varphi_0 - \frac{\lambda}{2}\sin\frac{\varphi_0}{2}\sigma_{x2}. \tag{63}$$

It follows from these equations that indeed the phases across the coupling JJ and the second measurement JJ remain negligibly small even though the first measurement junction may be biased at the critical level. Thus, the constraint (20) is essential for not disturbing the other qubit while the first qubit is measured.

3.2. Qubit coupling via read-out junctions

In the case of qubit–qubit coupling, both measurement junctions are biased, while the coupling junction is not tilted by external bias,

$$\sin\varphi_{mi,0} = \frac{\hbar}{2e}\frac{I_{mi}}{E_{Ji}^m}, \quad \varphi_0 = 0. \tag{64}$$

Expanding the potential terms in equations (60)–(62) around the steady state point up to second order with respect to small phase fluctuations, γ and $\gamma_{mi} = \varphi_{mi} - \varphi_{mi,0}$, and neglecting β-corrections, we may present the Hamiltonian in the form

$$H = \sum_{i=1}^{2} H_i + H_{\rm osc} + H_{\rm int}. \tag{65}$$

Here

$$H_i = \frac{E_C}{2}(1 - 2n_{gi})\sigma_{zi} - E_J\cos\frac{\varphi_{mi,0}}{2}\,\sigma_{xi}, \tag{66}$$

is the qubit Hamiltonian, which differs from the one in equation (11) by the phase of the measurement JJ substituting for the phase of the coupling JJ. The next term,

$$H_{\rm osc} = E_C^b n^2 + E_{C1}^m n_{m1}^2 + E_{C2}^m n_{m2}^2 + \tfrac{1}{2}(E_J^b\gamma^2 + E_{J1}^m\cos\varphi_{m1,0}\gamma_{m1}^2 + E_{J2}^m\cos\varphi_{m2,0}\gamma_{m2}^2) \tag{67}$$

describes uncoupled linear oscillators, while the interaction is described by the last term,

$$\begin{aligned} H_{\rm int} = {} & \tfrac{1}{2}\lambda E_J^b[(\Delta_1 + \Delta_2)\gamma^2 + \Delta_1\gamma_{m1}^2 + \Delta_2\gamma_{m2}^2] + \lambda E_J^b(\Delta_2\gamma_{m2} - \Delta_1\gamma_{m1})\gamma \\ & + \lambda E_J^b[(B_1 - B_2)\gamma - B_1\gamma_{m1} - B_2\gamma_{m2}]. \end{aligned} \tag{68}$$

Here we introduced for brevity the following notations,

$$\Delta_i = \tfrac{1}{4}\cos\frac{\varphi_{mi,0}}{2}\sigma_{xi}, \qquad B_i = -\tfrac{1}{2}\sin\frac{\varphi_{mi,0}}{2}\sigma_{xi}. \tag{69}$$

Now our goal will be to eliminate the linear terms in γs in equation (68), which can be easily done by using oscillator normal modes. To this end we rewrite the potential part of equations (67) and (68) in a symbolic form in terms of a 3-vector $\hat\gamma = (\gamma, \gamma_{m1}, \gamma_{m2})$,

$$\tfrac{1}{2}E_J^b\hat\gamma(\hat D + \lambda\hat\Delta)\hat\gamma + \lambda E_J^b\hat B\hat\gamma. \tag{70}$$

Here $\hat{D}$ is a diagonal matrix representing the free oscillator potentials in equation (67), while the 3×3 matrix $\hat{\Delta}$ and the 3-vector $\hat{B}$ represent the interaction in equations (68) and (69). Without loss of generality we may assume the charging energies of the oscillators to be equal.[2] Then performing rotation to the eigenbasis $\hat{\gamma}'$ of the matrix $\hat{D} + \lambda\hat{\Delta}$ and then shifting the variable, $\tilde{\gamma} = \hat{\gamma}' + \lambda\hat{D}'^{-1}\hat{B}'$ (here the prime indicates a new basis), we get,

$$\tfrac{1}{2}E_J^b\tilde{\gamma}\hat{D}'\tilde{\gamma} - \tfrac{1}{2}\lambda^2 E_J^b\hat{B}(\hat{D} + \lambda\hat{\Delta})^{-1}\hat{B}. \tag{71}$$

The last term in this equation, which is conveniently written in the original basis, gives a direct controllable qubit–qubit coupling similar to the one in equation (22),

$$H_{\text{int}} = \frac{1}{4}\lambda E_J \sin\frac{\varphi_{m1,0}}{2}\sin\frac{\varphi_{m2,0}}{2}\sigma_{x1}\sigma_{x2}. \tag{72}$$

As expected, this coupling is switched off when one or both measurement junctions are idle, and it is switched on only when both the measurement junctions are biased. We emphasize that this coupling does not require biasing of the coupling junction.

The first term in equation (71) gives, after averaging over the oscillator ground state, the oscillator ground state energy, $(\hbar\omega_b/2)\,\text{Tr}\sqrt{\hat{D}'}$ (remember that $\hat{D}'$ is diagonal). Treating $\lambda\hat{\Delta}$ as a small perturbation, we find the first perturbative correction to the matrix spectrum, $\hat{D}' = \hat{D} + \lambda\,\text{diag}\,\hat{\Delta}$. It is easy to see that only the contribution of the coupling JJ contains the dependence on the qubit-state configuration. The relevant matrix element has the explicit form $(1/2)E_J^b\,[1 + \lambda(\Delta_1 + \Delta_2)]$, and yields the residual interaction

$$H_{ires} = -\frac{1}{128}\lambda E_J\frac{\hbar\omega_b}{E_J^b}\cos\frac{\varphi_{m1,0}}{2}\cos\frac{\varphi_{m2,0}}{2}\sigma_{x1}\sigma_{x2}. \tag{73}$$

This is a small residual interaction substituting for equation (32) in the present case.

4. Multi-qubit network

To implement useful quantum algorithms, controllable systems with large numbers of qubits are needed. In this section we will show that the effective qubit–qubit coupling derived in sections 2 and 3 can be generalized to a chain of N qubits with each qubit being coupled to its nearest neighbours via current-biased JJs and each having its own read-out device, as shown in figure 3.

4.1. Circuit Hamiltonian

The Lagrangian of the N-qubit circuit presented in figure 3 can be written as a straightforward generalization of equations (2)–(4), and (55),

$$L = \sum_{i=1}^{N}[L_{\text{SCB},i} + L_{mi}] + \sum_{i=1}^{N-1}L_{JJ,i}. \tag{74}$$

[2] By rescaling γ-variables, the charging energies can always be made equal; then rescaling constant factors will appear in Δ_i and B_i, introducing no qualitative changes.

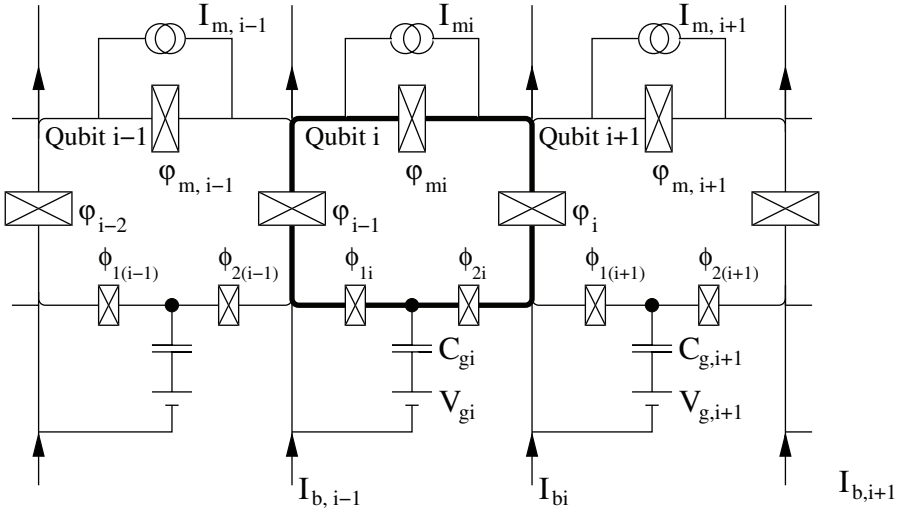

Figure 3. A system of N coupled charge qubits. V_{gi} controls individual qubit i, whereas I_{bi} controls the coupling of qubits i and $i+1$. I_{mi} can be used to read out the current state of qubit i and also for qubit coupling. There are no coupling JJs at the ends, $\varphi_0 = \varphi_N = 0$. Directions of the Josephson currents are the same as indicated by the arrows in figure 2.

Since now there are two coupling JJs per qubit loop, the flux quantization relation (56) must be extended,

$$\phi_{+,i} + \varphi_i - \phi_{mi} - \varphi_{i-1} = 0, \tag{75}$$

leading to a more complex form of the interaction among the qubits and the coupling and measurement JJs. Nevertheless, our previous strategy for elimination of the interaction in the charge sector still works. Generalizing equation (57),

$$\phi_{-,i} \to \phi_{-,i} + 2\alpha(\varphi_{mi} + \varphi_{i-1} + \varphi_i) \tag{76}$$

allows us to decouple qubit charges; the resulting weak interaction in the current sector yields a direct parasitic yy-qubit coupling, similar to the one in equation (30). Further transformation, generalizing equation (58),

$$\varphi_{mi} \to \varphi_{mi} + \beta(\varphi_i - \varphi_{i-1}), \qquad \beta = \frac{C}{2C_{mi} + C}, \tag{77}$$

decouples the charges of the measurement JJs, and yields weak additional interaction in the current sector, which will also be omitted.

After the transformations (76) and (77), the only capacitive interaction which remains in the Lagrangian (74) is the interaction among the coupling JJs. This interaction is proportional to a small qubit capacitance C, while the diagonal terms are proportional to much larger capacitances of the coupling JJs, $C_{bi} \gg C$. We assume that the JJ capacitances are different so that $C_{bi} - C_{bj} \gg C$; this is a realistic assumption because a spread of the junction characteristics during fabrication usually exceeds 10%. Under this assumption, the diagonalization of the

capacitance matrix will introduce small corrections to the inductive interaction, corrections which will not provide any qualitative change and can be omitted.

With diagonal kinetic terms in the Lagrangian (74), it is straightforward to proceed to the truncation of the quantum Hamiltonian,

$$H = \sum_{i=1}^{N} [H_i + H_{mi}] + \sum_{i=1}^{N-1} H_{JJ,i}. \tag{78}$$

In the charge regime, $E_J \ll E_C$, the qubit Hamiltonian will take the form,

$$H_i = \frac{E_C}{2}(1 - 2n_{gi})\sigma_{zi} - E_J \cos\frac{\varphi_i - \varphi_{mi} - \varphi_{i-1}}{2}\sigma_{xi}, \tag{79}$$

while the large-JJ terms will not change,

$$\begin{aligned} H_{mi} &= E^m_{Ci} n^2_{mi} - E^m_{Ji}\cos\varphi_{mi} - \frac{\hbar}{2e} I_{mi}\varphi_{mi}, \\ H_{JJ,i} &= E^b_C n^2_i - E^b_J \cos\varphi_i - \frac{\hbar}{2e} I_{bi}\varphi_i. \end{aligned} \tag{80}$$

In these equations, the effective capacitances of the measurement JJs are the same as in equation (65), while the effective capacitances of the coupling JJs are straightforward generalizations of the one in equation (62), namely $C_{b\Sigma,i} = C_b + C[(C_{mi} + C)/(2C_{mi} + C) + (C_{m,i+1} + C)/(2C_{m,i+1} + C)]$.

4.2. Direct qubit–qubit coupling

The next step in the derivation of the direct qubit–qubit coupling is to eliminate the large JJs, following the previous procedure for the two-qubit case. After expanding the Hamiltonian, equations (78)–(80), with respect to small fluctuations around the steady state points, $(\varphi_{i0}, \varphi_{mi,0})$, determined by the applied controlling and measurement currents,

$$\sin\varphi_{mi,0} = \frac{\hbar}{2e}\frac{I_{mi}}{E^m_{Ji}}, \qquad \sin\varphi_{i0} = \frac{\hbar}{2e}\frac{I_{bi}}{E^b_J}, \tag{81}$$

we get the qubit terms (79) with steady-state phases, (81), in the Josephson terms. The qubits interact with a subnetwork of the linear oscillators,

$$H_{\rm osc} = \sum_{i=1}^{N-1}\left[E^b_C n^2_i + \frac{E^b_J}{2}\cos\varphi_{i0}\gamma^2_i\right] + \sum_{i=1}^{N}\left[E^m_{Ci} n^2_{mi} + \frac{E^b_J}{2}\cos\phi_{mi0}\gamma^2_{mi}\right], \tag{82}$$

via the interaction Hamiltonian, which also connects the oscillators,

$$\begin{aligned} H_{\rm int} = {} & \frac{\lambda E^b_J}{2}\sum_{i=1}^{N-1}[(\Delta_i + \Delta_{i+1})\gamma^2_i - 2\Delta_i\gamma_i\gamma_{i-1}] \\ & + \frac{\lambda E^b_J}{2}\left[\sum_{i=1}^{N}\Delta_i\gamma^2_{mi} + 2\sum_{i=1}^{N-1}(\Delta_i\gamma_i\gamma_{mi} - \Delta_{i+1}\gamma_i\gamma_{m,i+1})\right] \\ & + \lambda E^b_J\left[\sum_{i=1}^{N-1}(B_i - B_{i+1})\gamma_i - \sum_{i=1}^{N} B_i\gamma_{mi}\right]. \end{aligned} \tag{83}$$

The quantities Δ and B now also contain the phases of the two coupling JJs (cf equation (69)),

$$\Delta_i = \tfrac{1}{4}\cos\frac{\varphi_{i0} - \phi_{mi0} - \varphi_{i-1,0}}{2}\sigma_{xi},$$
$$B_i = \tfrac{1}{2}\sin\frac{\varphi_{i0} - \phi_{mi0} - \varphi_{i-1,0}}{2}\sigma_{xi}. \tag{84}$$

The interaction (83) can be presented in the symbolic form of equation (70) by introducing the $(2N-1)$-vector $\hat{\gamma} = (\gamma_1, \gamma_2, \ldots, \gamma_{m1}, \gamma_{m2}, \ldots)$, the $(2N-1)\times(2N-1)$ matrix $\hat{\Delta}$ representing the oscillator interaction, and the $(2N-1)$-vector $\hat{B}$ representing the qubit–oscillator interaction. Then we proceed to equation (71) by performing the diagonalization, and shifting the oscillator variables as described after equation (70). The result of this procedure is as follows [22]: assuming no applied measurement currents, the coupling induced by only tilting coupling JJs has the form,

$$H_{\rm int} = \sum_{i=1}^{N-1} \frac{\lambda E_J}{4\cos\varphi_{i0}} \sin\frac{\varphi_{i0} - \varphi_{i-1,0}}{2} \sin\frac{\varphi_{i+1,0} - \varphi_{i0}}{2}\sigma_{xi}\sigma_{x,i+1}. \tag{85}$$

On the other hand, when the coupling JJs are kept idle while the measurement junctions are biased, the coupling has the form,

$$H_{\rm int} = \sum_{i=1}^{N-1} \frac{\lambda E_J}{4} \sin\frac{\phi_{mi0}}{2} \sin\frac{\phi_{m,i+1,0}}{2}\sigma_{xi}\sigma_{x,i+1}. \tag{86}$$

Whichever way the coupling is initiated, one is allowed to simultaneously perform a number of two-qubit gates on different qubit pairs, as long as the qubit pairs are separated by at least one idle qubit. The small residual xx-coupling resulting from the shift of the oscillators' ground energy is restricted to the neighbouring qubits and given by equation (32).

We conclude this section with a discussion of the effect of different Josephson energies of the qubit junctions, E_{Ji}, and the coupling JJ, E^b_{Ji}. This variation can easily be taken into account by introducing numerical scaling factors, $E_{Ji} = \xi_i E_J$, and $E^b_{Ji} = \xi^b_i E^b_J$. Then, while deriving equation (83), these scaling factors can be included in the definition of the quantities Δ_i and B_i in equation (84). As a result, the coupling energies λE_J in the final results, equations (85) and (86), are replaced by

$$\lambda E_J = \frac{E_J^2}{E^b_J} \to \frac{E_{Ji}E_{Ji+1}}{E^b_{Ji}}. \tag{87}$$

5. Gate operations with the qubit network

All quantum algorithms can be implemented using a limited universal set of gates. One such set consists of the controlled-NOT (CNOT) gate together with single-qubit gates [32]. In this section, we will describe how to perform a CNOT gate on two neighbouring qubits in the above-mentioned charge qubit network. Using a sequence of two-qubit operations on nearest neighbours only, two-qubit operations on arbitrary qubits in the chain can be performed [12]. The CNOT

gate presented here is composed of a CPHASE gate and two kinds of single-qubit gates, a phase gate and the Hadamard gate.

By default, during qubit operations the qubits are parked at the charge degeneracy point, where they are more stable against charge noise [3, 23] and the qubit levels are maximally separated from higher states. The computational basis is chosen to be the current basis, which is the eigenbasis at the charge degeneracy point and differs from the charge basis by the rotation $\sigma_x \leftrightarrow \sigma_z$.

5.1. Single-qubit operations

When $I_{bi} = I_{b,i-1} = I_{mi} = 0$, qubit i is disconnected from the network to first-order and single-qubit gates can be performed. The time evolution is determined by the single-qubit Hamiltonian H_i, equation (16) or (66),

$$H_i = E_C \delta n_{gi}(t)\sigma_{xi} - E_J \sigma_{zi}, \tag{88}$$

where $\delta n_{gi}(t) = 1/2 - n_{gi}(t)$ is the deviation from the charge degeneracy point.

In the idle state, the non-zero energy-level splitting results in a phase gate S_θ being performed on the qubit;

$$\mathrm{S}_\theta = \begin{cases} |0\rangle & \rightarrow \quad \mathrm{e}^{\mathrm{i}\theta/2}|0\rangle, \\ |1\rangle & \rightarrow \quad \mathrm{e}^{-\mathrm{i}\theta/2}|1\rangle, \end{cases} \tag{89}$$

where θ depends on the elapsed time T through $T = \theta/(2E_J)$.

A particularly useful case is the Z-gate, equivalent to the $S_{3\pi/2}$-gate (up to a global phase),

$$\mathrm{Z} = \begin{cases} |0\rangle & \rightarrow \quad |0\rangle, \\ |1\rangle & \rightarrow \quad \mathrm{i}|1\rangle. \end{cases} \tag{90}$$

Another useful single-qubit operation is the Hadamard gate H,

$$\mathrm{H} = \begin{cases} |0\rangle & \rightarrow \quad \frac{1}{\sqrt{2}}(|0\rangle + |1\rangle), \\ |1\rangle & \rightarrow \quad \frac{1}{\sqrt{2}}(|0\rangle - |1\rangle), \end{cases} \tag{91}$$

which can be implemented by applying a microwave pulse at the gate [3, 31], $\delta n_{gi}(t) = A\cos(2E_J t)$, during a time $T = \pi/2A$. Choosing the amplitude A involves a trade-off between keeping the operation time short and minimizing the deviations from the charge degeneracy point.

5.2. Two-qubit gates

A two-qubit gate involving qubits i and $i+1$ is created by applying a bias current I_{bi} at the intersection between the two qubits, or by simultaneously applying measurement currents I_{mi} and $I_{m,i+1}$. The qubits are coupled according to the coupling terms equations (85) and (86), while their individual time evolutions are determined by H_i, equation (16) or (66). As an example, when applying the bias current I_{bi}, the Hamiltonian of the two interacting qubits reads,

$$H_i + H_{i+1} + H_{\mathrm{int}} = -E_J \cos\frac{\varphi_{i0}}{2}(\sigma_{zi} + \sigma_{z,i+1}) - \frac{\lambda E_J}{4\cos\varphi_{i0}} \sin^2\frac{\varphi_{i0}}{2}\sigma_{zi}\sigma_{z,i+1}. \tag{92}$$

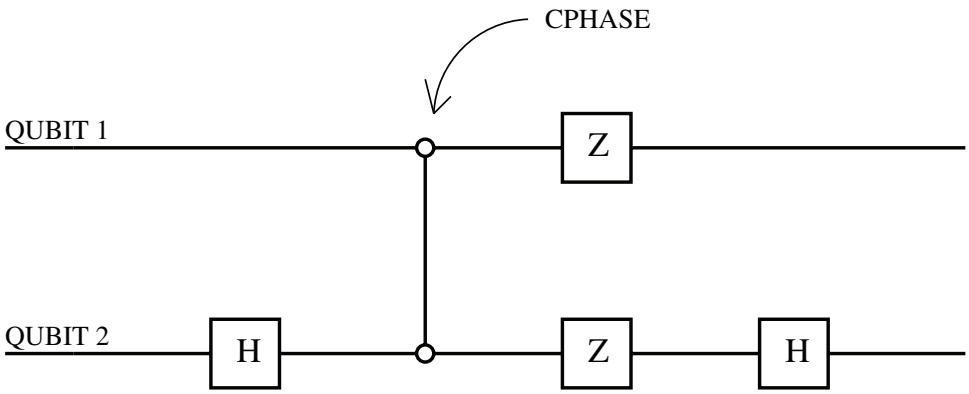

Figure 4. A CNOT operation using single-qubit gates (Hadamard and phase gates) and CPHASE. Time runs from left to right.

Choosing operation time and bias current amplitude properly results in the entangling CPHASE gate,

$$\text{CPHASE} = \begin{cases} |11\rangle & \rightarrow & \mathrm{i}|11\rangle, \\ |10\rangle & \rightarrow & |10\rangle, \\ |01\rangle & \rightarrow & |01\rangle, \\ |00\rangle & \rightarrow & \mathrm{i}|00\rangle. \end{cases} \tag{93}$$

Moreover, a CNOT gate is created by combining CPHASE with single-qubit gates such as the Z-gate, equation (90), and the Hadamard gate, equation (91), as shown in figure 4. Thus it is possible to perform a universal set of quantum gates, and therefore any quantum algorithm, with the investigated charge-qubit network.

Acknowledgments

The authors acknowledge useful discussions with D Esteve and Yu Makhlin. The support from EU-SQUBIT2 and Swedish grant agencies SSF and VR are gratefully acknowledged.

References

[1] Nakamura Y, Pashkin Yu A and Tsai J S 1999 *Nature* **398** 786
[2] van der Wal C H, ter Haar A C J, Wilhelm F K, Schouten R N, Harmans C J P M, Orlando T P, Lloyd S and Mooij J E 2000 *Science* **290** 773
[3] Vion D, Cottet A, Aassime A, Joyez P, Pothier H, Urbina C, Esteve D and Devoret M H 2002 *Science* **296** 886
[4] Martinis J M, Nam S, Aumentado J and Urbina C 2002 *Phys. Rev. Lett.* **89** 117901
[5] Chiorescu I, Nakamura Y, Harmans C J P M and Mooij J E 2003 *Science* **299** 1869
[6] Collin E, Ithier G, Aassime A, Joyez P, Vion D and Esteve D 2004 *Phys. Rev. Lett.* **93** 157005
[7] Pashkin Yu A, Yamamoto T, Astafiev O, Nakamura Y, Averin D V and Tsai J S 2003 *Nature* **421** 823
[8] Yamamoto T, Pashkin Yu A, Astafiev O, Nakamura Y and Tsai J S 2003 *Nature* **425** 941
[9] Berkley A J, Xu H, Ramos R C, Gubrud M A, Strauch F W, Johnson P R, Anderson J R, Dragt A J, Lobb C J and Wellstood F C 2003 *Science* **300** 1548

[10] Izmalkov A, Grajcar M, Il'ichev E, Wagner Th, Meyer H G, Smirnov A Yu, Amin M H S, Maassen van den Brink A and Zagoskin A M 2004 *Phys. Rev. Lett.* **93** 037003
[11] McDermott R, Simmonds R W, Steffen M, Cooper K B, Cicak K, Osborn K D, Oh S, Pappas D P and Martinis J M 2005 *Science* **307** 1299
[12] Schuch N and Siewert J 2003 *Phys. Rev. Lett.* **91** 027902
[13] Shnirman A, Schön G and Hermon Z 1997 *Phys. Rev. Lett.* **79** 2371
[14] Makhlin Yu, Schön G and Shnirman A 1999 *Nature* **398** 305
[15] Siewert J and Fazio R 2001 *Phys. Rev. Lett.* **87** 257905
[16] You J Q, Tsai J S and Nori F 2002 *Phys. Rev. Lett.* **89** 197902
[17] Plastina F and Falci G 2003 *Phys. Rev.* B **67** 224514
[18] Makhlin Yu, Schön G and Shnirman A 2001 *Rev. Mod. Phys.* **73** 357
[19] Blais A, Maassen van den Brink A and Zagoskin A M 2003 *Phys. Rev. Lett.* **90** 127901
[20] Averin D V and Bruder C 2003 *Phys. Rev. Lett.* **91** 057003
[21] You J Q, Tsai J S and Nori F 2003 *Phys. Rev.* B **68** 024510
[22] Lantz J, Wallquist M, Shumeiko V S and Wendin G 2004 *Phys. Rev.* B **70** 140507(R)
[23] Duty T, Gunnarsson D, Bladh K and Delsing P 2004 *Phys. Rev.* B **69** 140503(R)
[24] Zorin A 2002 *Physica* C **368** 284
[25] Devoret M 1997 *Quantum Fluctuations in Electrical Circuits* (Les Houches LXIII, 1995) (Amsterdam: Elsevier)
[26] Yurke B and Denker J S 1984 *Phys. Rev.* A **29** 1419
[27] Wang Y D, Zhang P, Zhou D L and Sun C P 2004 *Phys. Rev.* B **70** 224515
[28] Bender C M and Orszag S A 1999 *Advanced Mathematical Methods for Scientists and Engineers* (New York: Springer)
[29] Siddiqi I, Vijay R, Pierre F, Wilson C M, Metcalfe M, Rigetti C, Frunzio L and Devoret M H 2004 *Phys. Rev. Lett.* **93** 207002
[30] Weiss Y1999 *Quantum Dissipative Systems* 2nd edn (Hackensack, NJ: World Scientific) ch 12
[31] Nakamura Y, Pashkin Yu A and Tsai J S 2001 *Phys. Rev. Lett.* **87** 246601
[32] Barenco A, Bennett C H, Cleve R, DiVincenzo D P, Margolus N, Shor P, Sleator T, Smolin J A and Weinfurter H 1995 *Phys. Rev.* A **52** 3457